

High-temperature series for the B-site spinel and diamond lattices and the question of universality*

David N. Lambeth[†], M. Howard Lee,[‡] and H. Eugene Stanley

Department of Physics, Massachusetts Institute of Technology, Cambridge, Massachusetts 02139
(Received 4 June 1973)

The high-temperature series for the two-spin correlation functions on both the B-site spinel and diamond lattices have been calculated through tenth order for the Hamiltonian, $\mathcal{H} = -J \sum_{\langle ij \rangle} \sum_{\alpha=1}^{n(n \leq D)} S_i^\alpha S_j^\alpha$. Here S_i^α is the α th component of the D -dimensional classical spin and we define n as the spin space symmetry parameter. By $\langle ij \rangle$ we limit the first summation to nearest-neighbor pairs of sites i and j on the lattice. The spin space symmetry parameter n is $\leq D$. We consider all six models resulting from $D = 1-3$. Our analysis of the high-temperature series indicates that while the exponent estimates for the more loosely packed diamond lattice ($q = 4$) indicate agreement with the universality hypothesis, the B-site spinel lattice ($q = 6$) series are not yet displaying their critical behavior. Some conjectures concerning this peculiarity of the series for the two lattices are made.

I. INTRODUCTION

One aspect of the universality hypothesis¹ in critical phenomena is that for a given spatial dimension d the critical exponents for a given Hamiltonian should be independent of lattice structure. Existing evidence² indicates that for lattices with "simple" cubic symmetry³ [e.g., simple cubic (sc), body centered cubic (bcc), and face centered cubic (fcc)] critical exponents are indeed independent of lattice structure.

Stanley and Kaplan⁴ observed, however, that sixth-order high-temperature series (HTS) for the magnetic susceptibility of the Heisenberg model on the B-site spinel lattice did not support the "universal" $D = 3$ value of $\gamma \cong 1.4$. They suggested that γ might be as small as $\cong 1$. One year later Jasnow and Moore⁵ extended the classical Heisenberg model series and also obtained new series for the $s = \frac{1}{2}$ Ising model⁶ and classical X-Y model to eighth order on the B-site spinel lattice. They noted, as did Stanley and Kaplan, that a six-term ratio plot has become flat indicating an exponent of $\gamma \cong 1$, but with the addition of their two new terms the ratios were bending downward indicating that γ might possibly be increasing.

In the present study we calculate tenth-order HTS on both the B-site spinel lattice and the more familiar diamond lattice.⁷ In Sec. II the two lattices are compared and in Sec. III the six different models considered are described. Analysis of the series is presented in Sec. IV and in Sec. V our conclusions are given.

II. THE LATTICE STRUCTURES

A. B-site spinel lattice

The discovery of certain insulating ferromagnetic materials⁸ such as CdCr_2Se_4 , CdCr_2S_4 , and HgCr_2Se_4 and the antiferromagnets HgCr_2S_4 , ZnCr_2Se_4 , and ZnCr_2S_4 have stimulated an interest in the spinel structure. The structure is described by the formula AB_2X_4 where the A sites are occupied by diamagnetic ions, the B sites by magnetic ions, and the X sites by nonmagnetic ions. We model materials for which there are significant magnetic interactions among only the B sites.

We will assume these interactions are nearest neighbor only (see Ref. 8).

The B-site spinel lattice can be understood in terms of its four sublattice structure.⁹ Consider a cubic unit cell of the fcc structure with unit cell length being $4a$. The B sites of the spinel lattice will then result if one superimposes three similar fcc lattices with their origins located at $a(1, 1, 0)$, $a(1, 0, 1)$, and $a(0, 1, 1)$. From Fig. 1¹⁰ we see that each B site (the unfilled circles) has six nearest neighbors ($q = 6$) and that these neighbors are placed at the corners of a pair of triangular pyramids joined at the site. Hence, the lattice can be considered as loosely packed since it consists of only half the sites of an fcc lattice, but it can also be considered as tightly packed since nearest-neighbor (nn) lattice sites have common nearest neighbors. This means that, in the language of graph theory, graphs composed of triangles will contribute at lower order in the HTS for the B-site spinel lattice than they will in the HTS for the sc or bcc lattices (traditionally considered more "tightly packed"). Yet the B-site spinel lattice allows a fewer total number of graphs because of the large regions of space void of any lattice sites (see, for example, the center portion of Fig. 1). That the asymptotic behavior is only slowly reached in the B-site spinel lattice, we suspect, lies in this peculiarity of the lattice structure of allowing graphs which normally only fit on tightly packed lattices and yet of not allowing a great many chainlike graphs.

B. Diamond lattice

The diamond lattice can also be constructed in terms of fcc sublattices. Consider an fcc lattice of unit cell length $4a$. The diamond lattice will then result if one superimposes an additional fcc lattice with its origin located at $a(1, 1, 1)$. Each site then has 4 nn ($q = 4$) and it is located at the center of a tetrahedron. This lattice cannot be considered, in any sense, tightly packed. In fact in doing a "self-avoiding walk" on the lattice, it is impossible to form a closed loop in fewer than six steps.¹¹ The diamond lattice is obtained from Fig. 1 if only the solid circles are observed.⁷

TABLE I. A, Summary of previous work and comparison with present work. $C_2(r)$ denotes the pair correlation function from which $\bar{\chi}$, μ_2 and \bar{C}_H follow immediately. B, The names of the six models are given according to the dimensionality of the spin space D and the spin space symmetry number n . Our estimates for the critical values using all analysis are listed. The estimate of the critical temperature for the $S=\frac{1}{2}$ Ising model on the diamond lattice is from Ref. 7.

A							
B-site spinel				Diamond			
Order	Range of n, D	Function calculated	Ref.	Order	Range of n, D	Function calculated	Ref.
6	$n=D=3$	$\bar{\chi}$ only	4	16	$n=D=1$	many functions but not $C_2(r)$	7
8	$n=D=1$; $n=2, D=3$; $n=D=3$	$C_2(r)$	5				
10	$n=D=1$	$\bar{\chi}, \bar{C}_H$	6				
16	$n=D=1$	C_H	12				
Six cases:				Six cases:			
10	all n with $n \leq D$ and $D=1, 2, 3$	$C_2(r)$	this work	10	all n with $n \leq D$ and $D=1, 2, 3$	$C_2(r)$	this work

B						
D	n	Model	K_c/K_c^{MF}	Diamond		B-site spinel
				γ	$2\nu + \gamma$	K_c/K_c^{MF}
1	1	Ising ($S=\frac{1}{2}$)	1.4793 ± 0.0002	1.25 ± 0.02	2.55 ± 0.05	1.42 ± 0.01
2	1	$D=2$, Ising	1.358 ± 0.002	1.25 ± 0.01	2.53 ± 0.01	1.32 ± 0.01
2	2	Planar	1.540 ± 0.005	1.34 ± 0.02	2.70 ± 0.05	1.48 ± 0.02
3	1	Ising ($S=\infty$)	1.290 ± 0.0005	1.25 ± 0.005	2.53 ± 0.005	1.26 ± 0.005
3	2	X-Y	1.420 ± 0.005	1.33 ± 0.02	2.67 ± 0.03	1.38 ± 0.01
3	3	Heisenberg	1.575 ± 0.005	1.41 ± 0.01	2.70 ± 0.2	1.52 ± 0.02

It is obvious from Fig. 1 that there is a great deal of similarity between the diamond and the B-site spinel lattices. Gibberd first exploited this similarity.¹² By a transformation technique, he was able to extend the $s=\frac{1}{2}$ Ising model specific heat HTS to 16th order on the cristobalite^{6,7} lattice using the series for the diamond lattice. (For our purposes the cristobalite and the B-site spinel lattices are the same—see Refs. 6 and 10.)

III. MODELS AND SERIES

We define the interaction Hamiltonian as

$$\mathcal{H} = -J \sum_{\langle ij \rangle} \sum_{\alpha=1}^n (n \leq D) S_i^\alpha S_j^\alpha, \quad (3.1)$$

where S_i^α is the α th component of the D -dimensional classical spin located at the i th site. The first sum is over nn pairs of lattice sites while the second sum is over the components of the spin. The parameter $n(n \leq D)$ will be referred to as the spin space symmetry parameter, since universality would predict common values of exponents for common values of n . Our expression [Eq. (3.1)] is a slightly generalized version of the usually considered Hamiltonian. In order to avoid confusion we present the model names associated with the parameters n and D in the first part of Table I. B. We treat the

model for $D=2, n=1$ simply to give a sense of completeness to the present work.

Using a computer program based upon the renormalized linked-cluster theory of Wortis *et al.*,¹³ we have obtained HTS for the two-spin correlation functions¹⁴

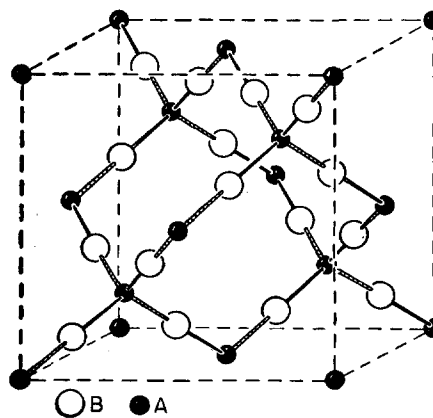


FIG. 1. The structure of the cristobalite lattice (AB_2). Here the unfilled circles represent the B sites of the spinel lattice while the filled circles form the diamond lattice.

TABLE II. The high-temperature series coefficients for the reduced susceptibility, $\bar{\chi}$, second moment, μ_2 , and the reduced specific heat, \bar{C}_H , on the B-site spinel lattice are: (a), Ising ($S=1/2$) model; (b), $D=2$, Ising model; (c), planar model; (d), Ising ($S=\infty$) model; (e), X-Y model; (f), Heisenberg model.

	$\bar{\chi}$	μ_2	\bar{C}_H		$\bar{\chi}$	μ_2	\bar{C}_H
a	Ising ($S=1/2$)			b	$D=2$ Ising		
0	1.0000	0.0	0.0	0	1.0000	0.0	0.0
1	6.0000	6.0000	3.0000	1	6.0000	6.0000	3.0000
2	30.0000	72.0000	12.0000	2	31.5000	72.0000	12.0000
3	136.0000	580.0000	15.0000	3	155.2500	596.2500	39.3750
4	598.0000	3864.0000	-40.0000	4	745.5000	4171.5000	105.0000
5	2628.8000	23088.8000	-148.0000	5	3541.2500	26502.1250	257.1875
6	11565.3333	128971.2000	313.6000	6	16727.3906	158307.8750	840.0000
7	50703.8762	688926.4762	4425.6667	7	78718.6738	906423.7832	4455.9443
8	220989.6952	3565320.2286	20716.9524	8	369152.1081	5033000.9284	24946.9323
9	957169.2106	18014889.1471	56633.4476	9	1725131.9227	27301997.9184	120227.3312
10	4128674.7613	89309944.5699	77235.6960	10	8037097.9292	145404666.0129	505611.2916
c	Planar			d	Ising ($S=\infty$)		
0	1.0000	0.0	0.0	0	1.0000	0.0	0.0
1	6.0000	6.0000	3.0000	1	6.0000	6.0000	3.0000
2	30.0000	72.0000	12.0000	2	32.4000	72.0000	12.0000
3	135.0000	570.0000	13.5000	3	167.0400	606.2400	54.3600
4	582.0000	3834.0000	-60.0000	4	841.6800	4363.2000	196.8000
5	2492.0000	22646.0000	-242.5000	5	4188.7190	28706.0356	647.0890
6	10683.5000	124463.0000	210.0000	6	20700.8758	178206.3713	2255.2869
7	45732.6250	652171.6250	5026.4375	7	101859.0454	1062511.9065	9168.5835
8	194221.6667	3304705.4167	22107.6667	8	499506.5556	6150315.9830	41988.2776
9	817617.5333	16329057.1167	42378.3375	9	2442372.0146	34805908.7648	199105.2876
10	3419942.0589	79074458.2337	-52837.5815	10	11911548.7638	193492861.9353	927675.0581
e	X-Y			f	Heisenberg		
0	1.0000	0.0	0.0	0	1.0000	0.0	0.0
1	6.0000	6.0000	3.0000	1	6.0000	6.0000	3.0000
2	31.2000	72.0000	12.0000	2	30.0000	72.0000	12.0000
3	150.7200	592.3200	33.4800	3	134.4000	578.4000	12.6000
4	703.6800	4089.6000	62.4000	4	572.4000	3816.0000	-72.0000
5	3237.8096	25497.2473	59.1184	5	2409.3257	22379.7257	-300.6857
6	14799.9791	148841.2212	152.2286	6	10159.9543	121748.4343	149.7600
7	67371.1715	830422.9256	2469.8201	7	42793.7829	630120.4114	5570.0400
8	305404.4177	4483986.0433	18821.1989	8	178816.1368	3149863.9151	23923.8661
9	1378116.5925	23619399.2148	90460.0585	9	739096.0685	15341627.5839	34754.6965
10	6191866.8178	122006899.8256	319592.5468	10	3028914.0691	73179134.4345	-139875.2514

to tenth order in $K \equiv J/k_B T$ for all six models. The physical quantities such as the reduced susceptibility $\bar{\chi}$, the second moment μ_2 , and the reduced specific heat \bar{C}_H can all be obtained from the correlation functions $C_2(\mathbf{r})$,

$$\bar{\chi} \equiv \chi T k_B / N \mu^2 = \sum_{\mathbf{r}} C_2(\mathbf{r}), \quad (3.2)$$

$$\mu_2 = \sum_{\mathbf{r}} |\mathbf{r}|^2 C_2(\mathbf{r}), \quad (3.3)$$

and

$$\bar{C}_H \equiv C_H T / nN = -\frac{1}{2} T (\partial/\partial T) \sum_{\delta} C_2(\delta). \quad (3.4)$$

Here δ is the nn lattice vector. The HTS for these quantities for the B-site spinel lattice are given in Table II, and similarly the series for the six models on the diamond lattice are contained in Table III.¹⁵

IV. ANALYSIS OF SERIES

We have expressed the thermodynamic function, say $\bar{\chi}(K)$, in terms of a finite number of exact coefficients,

$$\bar{\chi} = \sum_l a_l K^l. \quad (4.1)$$

We shall assume that χ diverges near its critical temperature in a power law form with an exponent γ ,

$$\chi(T) \sim (T - T_c)^{-\gamma}, \quad T \rightarrow T_c^+. \quad (4.2)$$

Below we describe the principal methods of analysis of the series employed in the present work.¹⁶

A. Ratio test

For a power law singularity it is well known that the ratios of coefficients $\rho_l \equiv a_l / (a_{l-1} a_1)$ satisfy the relation,

$$\lim_{l \rightarrow \infty} \rho_l = (K_c^{MF} / K_c) \{1 + [(\gamma - 1)/l] + O(l^{-2})\}, \quad (4.3)$$

where $K_c^{MF} \equiv k_B / a_1 J$ is the critical temperature predicted by mean field theory. From Eq. (4.3) one can obtain both the critical temperature and exponent from the ratios in the asymptotic limit. In Figs. 2 and 3 we have plotted the ratios of the coefficients of the reduced susceptibility series vs $1/l$. Observe in both figures that for the three models with $n=D$ the ratio plots display the same general shape. In the case of the B-site spinel lattice, this is seen by the general flattening at $l=5$ and 6 and then the smooth bending over for higher orders. On the diamond lattice, similarities between the $n=D$

TABLE III. The high-temperature series coefficients for the reduced susceptibility, second moment, and the reduced specific heat on the diamond lattice are: (a), Ising ($S=1/2$) model; (b), $D=2$ Ising model; (c), planar model; (d), Ising ($S=\infty$) model; (e), X-Y model; (f), Heisenberg model.

	$\bar{\chi}$	μ_2	\bar{C}_H		$\bar{\chi}$	μ_2	\bar{C}_H
a				b			
Ising ($S=1/2$)				$D=2$, Ising			
0	1.0000	0.0	0.0	0	1.0000	0.0	0.0
1	4.0000	4.0000	2.0000	1	4.0000	4.0000	2.0000
2	12.0000	32.0000	0.0	2	13.0000	32.0000	0.0
3	34.6667	162.6667	-2.0000	3	41.5000	169.5000	8.2500
4	100.0000	682.6667	0.0	4	129.5000	760.0000	0.0
5	288.5333	2592.5333	61.3333	5	402.8333	3106.8333	65.8333
6	808.5333	9281.4222	0.0	6	1233.2917	11994.3333	0.0
7	2258.1841	31834.7175	-56.7556	7	3768.4701	44450.4701	401.3014
8	6307.2381	105734.5016	0.0	8	11434.0169	159891.5208	0.0
9	17599.3256	342716.6166	1884.3937	9	34654.2076	561956.1659	3004.2445
10	48686.6557	1090225.7823	0.0	10	104527.7569	1939471.6906	0.0
c				d			
Planar				Ising ($S=\infty$)			
0	1.0000	0.0	0.0	0	1.0000	0.0	0.0
1	4.0000	4.0000	2.0000	1	4.0000	4.0000	2.0000
2	12.0000	32.0000	0.0	2	13.6000	32.0000	0.0
3	34.0000	162.0000	-3.0000	3	45.7600	173.7600	14.6400
4	96.0000	672.0000	0.0	4	149.7829	808.9600	0.0
5	271.3333	2511.3333	63.3333	5	488.9273	3448.2873	101.5184
6	743.0000	8829.3333	0.0	6	1574.8362	13911.3953	0.0
7	2012.0833	29692.0833	-171.2083	7	5064.8900	53957.8138	787.3431
8	5462.5000	96481.3333	0.0	8	16169.5436	203389.9645	0.0
9	14828.3833	305441.7167	2117.8500	9	51573.7114	749702.1539	6255.6971
10	39791.3833	947985.0222	0.0	10	163739.7350	2715372.3149	0.0
e				f			
X-Y				Heisenberg			
0	1.0000	0.0	0.0	0	1.0000	0.0	0.0
1	4.0000	4.0000	2.0000	1	4.0000	4.0000	2.0000
2	12.8000	32.0000	0.0	2	12.0000	32.0000	0.0
3	39.6800	167.6800	5.5200	3	33.6000	161.6000	-3.6000
4	120.2286	737.2800	0.0	4	93.6000	665.6000	0.0
5	362.1878	2942.6678	51.0694	5	261.2571	2462.8571	65.1429
6	1071.9033	11060.9972	0.0	6	705.4629	8562.8343	0.0
7	3155.8541	39827.8269	222.1161	7	1873.3714	28449.0971	-241.6800
8	9227.8708	138930.3515	0.0	8	4992.6171	91195.9771	0.0
9	26911.7416	472836.0560	1712.4045	9	13326.8123	284479.0865	2399.0026
10	78077.3175	1578315.3196	0.0	10	35083.7951	869377.5138	0.0

curves are seen in the downward trend for $l = 5-7$, the upward trend for $l = 9$, and finally back downward at $l = 10$. The similarities in the peculiar shapes of these ratio plots suggest the loose packedness of the lattices.¹⁷ This irregular behavior of ratios makes it difficult to obtain estimates for the critical indices by the ratio method alone.

B. Padé approximants

Independent estimates for the critical temperature and exponent can be obtained by finding Padé approximants (PA's) to the logarithmic derivative of the series. Shown in Table IV are the estimates of the critical values given by the diagonal and near-diagonal elements of the PA's to the susceptibility and second moment series for the six different models on the two lattices. A comparison of these tables indicates that the estimates for the more loosely packed diamond lattice, surprisingly, appear more convergent than do those for the B-site spinel lattice.

For the diamond lattice the PA tables also indicate three additional singularities. There are a pair of complex conjugate singularities located at $K_c/K_c^{MF} \cong 0.1$

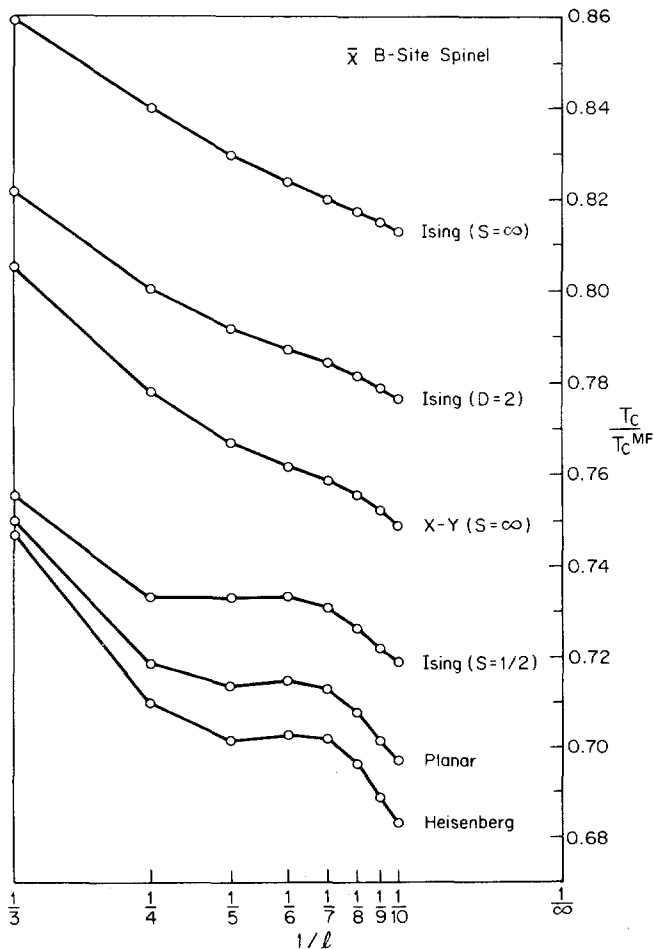


FIG. 2. The normalized ratios of coefficients $\rho_l \equiv a_l / (a_{l-1} a_1)$ for the susceptibility series (4.1) on the B-site spinel lattice. Note the similar trend for the ratios of coefficients where $n = D$.

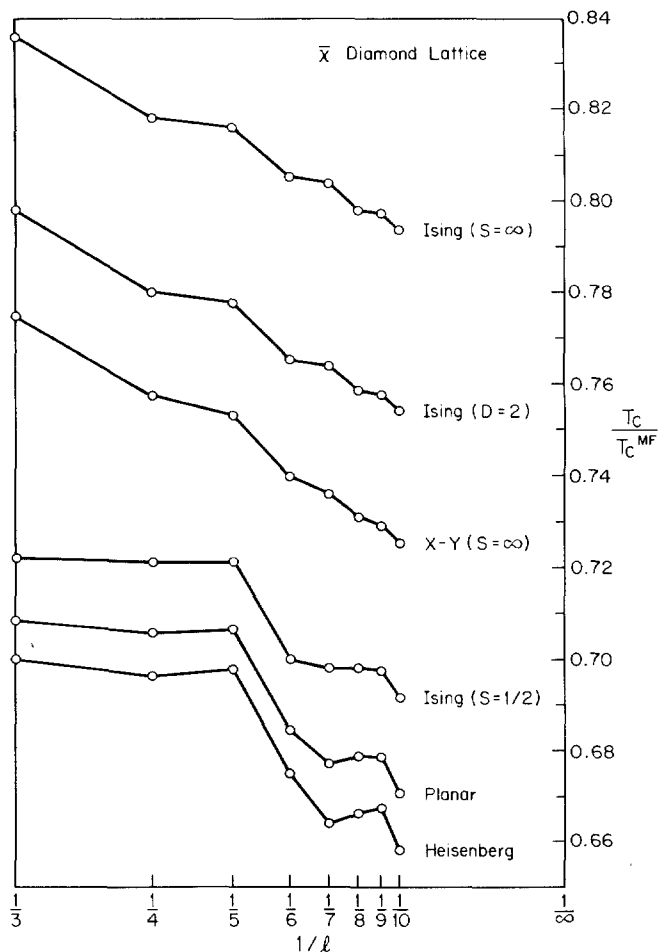


FIG. 3. The ratios of coefficient $\rho_l \equiv a_l / (a_{l-1} a_1)$ for the susceptibility series (4.1) on the diamond lattice.

$\pm (1.5) i$ and an antiferromagnetic singularity at about -1.5 . These three singularities consistently appear in the PA tables and occur with a strength (exponent) similar in magnitude to the ferromagnetic singularity. Thus, it is reasonable to believe that the PA's cannot accurately represent the ferromagnetic singularity until the order of the PA is sufficiently high to represent at least all four singularities. This is strikingly seen in Table IV,¹⁸ where the values of the PA's suddenly become convergent for D (order of the denominator) greater than or equal to four. The one exception is the $S = \infty$ Ising model series which seems to be represented by only the ferromagnetic and antiferromagnetic singularities.

The B-site spinel series also indicates a pair of complex conjugate singularities located at $K_c/K_c^{MF} \cong 1.5 \pm (1.5) i$. These do not, however, appear consistently throughout the Padé table and hence one does not see the sudden convergence to the ferromagnetic singularity.

C. Transformation methods

When there are nonphysical singularities located close to the physical singularity, it is sometimes possible to improve the estimates for the physical singularity by applying a transformation,¹⁹ thereby minimizing the effects of the nonphysical singularities. We have used the

TABLE IV. Estimates for the critical values by Padé approximants to the susceptibility and second moment series. N and D refer to the orders for the polynomials of the numerator and denominator, respectively, $K_c/K_c^{MF} = T_c^{MF}/T_c$. The models are: (a), Ising ($S=1/2$); (b), $D=2$, Ising; (c), planar; (d) Ising ($S=\infty$); (e), X-Y; (f), Heisenberg.

a					b				
Ising ($S=1/2$)					$D=2$, Ising				
Diamond		B-Site Spinel			Diamond		B-Site Spinel		
N, D	K_c/K_c^{MF}	γ	K_c/K_c^{MF}	γ	N, D	K_c/K_c^{MF}	γ	K_c/K_c^{MF}	γ
3,2	1.3846	0.9954	1.3915	1.1039	3,2	1.3498	1.2256	1.2955	1.1059
2,3	1.3807	0.9846	1.4057	1.1590	2,3	1.3408	1.1897	1.3057	1.1610
3,3	1.3040	0.8764	1.3904	1.0987	3,3	---	---	1.3030	1.1459
4,3	1.5116	1.4141	1.4633	1.5600	4,3	1.3640	1.2859	1.2904	1.0858
3,4	1.4818	1.2654	1.4008	1.1423	3,4	1.3576	1.2494	1.3054	1.1593
4,4	1.4827	1.2694	1.4524	1.4639	4,4	1.3593	1.2591	1.3397	1.4199
5,4	1.4796	1.2528	1.4662	1.5838	5,4	1.3594	1.2593	1.3152	1.2086
4,5	1.4820	1.2662	1.4273	1.2717	4,5	1.3594	1.2593	1.3194	1.2411
N, D		$2\nu+\gamma$		$2\nu+\gamma$	N, D		$2\nu+\gamma$		$2\nu+\gamma$
3,2	1.3881	2.0059	1.3598	1.9677	3,2	1.3466	2.4516	1.2961	2.2323
2,3	1.3795	1.9545	1.4090	2.3858	2,3	1.3428	2.4207	1.3041	2.3293
3,3	1.4271	2.2075	1.4000	2.3071	3,3	---	---	1.3076	2.3718
4,3	1.5016	2.7836	1.4803	3.5704	4,3	1.3621	2.5875	1.2817	2.1091
3,4	1.4813	2.5722	1.4067	2.3683	3,4	1.3571	2.5288	1.3034	2.3222
4,4	1.4815	2.5743	1.4458	2.8660	4,4	1.3588	2.5478	1.3272	2.6333
c					d				
Planar					Ising ($S=\infty$)				
3,2	1.3699	0.8841	1.3414	0.7944	3,2	1.2846	1.2236	1.4747	0.7816
2,3	1.3504	0.8365	1.4482	1.1939	2,3	1.2798	1.2035	1.5186	0.7058
3,3	1.4440	1.0485	1.4429	1.1730	3,3	1.2971	1.3046	1.2857	1.3452
4,3	1.5758	1.5344	1.4987	1.4765	4,3	1.2905	1.2534	1.2625	1.2498
3,4	1.5364	1.3345	1.4475	1.1917	3,4	1.2894	1.2454	1.2635	1.2565
4,4	1.5406	1.3528	1.5124	1.5818	4,4	1.2903	1.2515	1.2414	1.0738
5,4	1.5390	1.3442	1.5009	1.4904	5,4	1.2904	1.2523	1.2574	1.2175
4,5	1.5394	1.3471	1.4788	1.3330	4,5	1.2905	1.2535	1.2580	1.2222
3,2	1.3868	1.8336	1.3588	1.6833	3,2	1.2842	2.4676	1.3222	2.5863
2,3	1.1920	0.9823	1.4504	2.4323	2,3	1.2799	2.4315	1.4007	2.0650
3,3	1.4845	2.3431	1.4505	2.4330	3,3	1.2920	2.5602	1.2669	2.5691
4,3	1.5664	3.0218	1.4954	2.9363	4,3	1.2902	2.5321	1.2587	2.4780
3,4	1.5351	2.6061	1.4504	2.4323	3,4	1.2900	2.5294	1.2595	2.4901
4,4	1.5389	2.7308	1.4997	2.9982	4,4	1.2904	2.5354	1.2556	2.4307
e					f				
X-Y					Heisenberg				
3,2	1.4011	1.2522	1.3242	1.0258	3,2	1.3585	0.8159	1.3291	0.6835
2,3	1.3929	1.2201	1.3536	1.1810	2,3	1.1598	0.4586	1.4748	1.2115
3,3	---	---	1.3578	1.2028	3,3	1.4955	1.1305	1.4796	1.2300
4,3	1.4321	1.3832	1.4927	2.5604	4,3	1.6178	1.6140	1.5256	1.4643
3,4	1.4193	1.3112	1.3527	1.1776	3,4	1.5719	1.3800	1.4740	1.2092
4,4	1.4235	1.3335	1.3863	1.3752	4,4	1.5793	1.4127	1.5584	1.7142
5,4	1.4243	1.3382	1.3711	1.2607	5,4	1.5794	1.4134	1.5332	1.5095
4,5	1.4245	1.3401	1.3769	1.3065	4,5	1.5794	1.4134	1.5122	1.3656
3,2	1.3969	2.4921	1.3177	1.9713	3,2	1.3832	1.7202	1.3334	1.3567
2,3	1.3943	2.4717	1.3518	2.3636	2,3	2.0032	4.2933	1.4763	2.4532
3,3	1.3674	2.3535	1.3633	2.4899	3,3	1.5206	2.4306	1.4855	2.5285
4,3	1.4297	2.7758	1.4052	3.0543	4,3	1.6093	3.1839	1.5235	2.9229
3,4	1.4186	2.6473	1.3387	2.2618	3,4	1.5703	2.7784	1.4722	2.4296
4,4	1.4228	2.6928	1.3812	2.7029	4,4	1.5776	2.8447	1.5413	3.1747

following two transformations with limited success:

$$K \rightarrow K/[1 - (K/B)]$$

(4.4)

and

$$K \rightarrow K/[1 - (K/C)^2].$$

(4.5)

The first transformation, (4.4), is particularly useful in removing antiferromagnetic singularities, but it also maps complex singularities, such as those present in the spinel series, slightly farther from the origin. The second transformation, (4.5), has the property of stretching the imaginary axis of the complex K plane while keeping the real axis within the interval $[-C, C]$.

Both transformations seem to "straighten" the ratio plots for the spinel series. But we find that the exponents are rather sensitive to the transformation parameter. For this reason the transformations must be employed with care. The diamond lattice critical temperature estimates are only slightly improved by these transformations. This is because when the antiferromagnetic singularity is removed by transformation (4.4), the interference by the complex pair is enhanced. Similarly when transformation (4.5) is used, the antiferromagnetic singularity still remains strongly interfering.

Table I.B contains our estimates for the critical values for all the models. The diamond lattice exponents are all seen to be consistent with the universality values (i.e., they depend only on n). We are not able to obtain reasonable estimates for the B-site spinel lattice exponents, since the 10-term series is still too irregular to indicate its limiting behavior.

V. DISCUSSION AND CONCLUSIONS

In the present study we have considered HTS on two lattices which are considered loosely packed. Surprisingly, the series for the diamond lattice with the smaller coordination number ($q = 4$) appears to show its critical behavior much sooner than the series for the B-site spinel lattice with the higher coordination number ($q = 6$). This fact, we believe, is due to a peculiarity of the B-site spinel lattice. Because the lattice has a relatively large number of nearest neighbors which are common (tetrahedron shaped) and yet it has large regions of space void of any sites, the graphs which contribute near the origin are overweighted. Evidence supporting the idea that graphs of this type are dominating the behavior of the series is also contained in Gibberd's work.¹² In spite of his lengthy 16th-order *specific heat* series on the lattice, he could not obtain estimates for the exponent α . On the other hand our diamond lattice series appears to give much better convergence. This is, perhaps, a consequence of the fact that the graphs which extend farther from the origin play a more equal role relative to the graphs which reach only to the nearest neighbors.

In conclusion, we find that our estimates of the critical exponents for the diamond lattice (see Table I.B) agree with the values for the lattices with "simple" cubic symmetry³ (fcc, bcc, and sc). However, we cannot obtain estimates of the critical exponents for the B-site spinel lattice, since the series are still too irregular. Thus, we find that the universality hypothesis is upheld for the diamond lattice while we cannot find any evidence to contradict it for the B-site spinel lattice.

ACKNOWLEDGMENTS

We wish to thank F. Harbus and D. Karo for many stimulating discussions concerning the structure of the spinel lattice and Dr. D. D. Betts and Dr. R. V. Ditzian for comments concerning their work on the cristobalite lattice. We also wish to thank Dr. N. Menyuk and Dr. K. Dwight for a helpful discussion.

*Work supported by National Science Foundation, Office of Naval Research, and Air Force Office of Scientific Research.

[†]Work forms a portion of a Ph.D. thesis submitted to Kodak Park, Bldg. 81, Rochester, NY 14650.

[‡]Present address: Dept. of Physics and Astronomy, University of Georgia, Athens, Georgia 30602.

¹R. B. Griffiths, *Phys. Rev. Lett.* **24**, 1479 (1970), L. P. Kadanoff, in *Proceedings of the International School of Physics Enrico Fermi*, edited by M. S. Green (Academic, New York, 1971), p. 100.

²C. Domb and M. F. Sykes, *Phys. Rev.* **128**, 168 (1962).

³By "simple" cubic symmetry we mean that a lattice site has reflective symmetry about the Cartesian planes through one of the lattice sites. The B-site spinel and diamond lattices do not have this property.

⁴H. E. Stanley and T. A. Kaplan, *J. Appl. Phys.* **38**, 977 (1967).

⁵D. Jasnow and M. A. Moore, *Phys. Rev.* **176**, 751 (1968); the authors have given series for the susceptibility and second moment. For a description of the lattice see, also, D. Jasnow, Thesis, University of Illinois, Urbana, IL 1968.

⁶D. D. Betts and R. V. Ditzian, *Can. J. Phys.* **46**, 971 (1968). It should be noted that Betts and Ditzian had published tenth-order HTS for the partition function and the susceptibility for the $S = \frac{1}{2}$ Ising model series on the cristobalite lattice some 6 months before the work of Jasnow and Moore appeared. It was brought out in our discussion with D. D. Betts that the magnetic B sites of the AB_2X_4 spinel structure are identical to the magnetic B sites of the cristobalite lattice AB_2 . There is a slight disagreement in the tenth-order susceptibility coefficient between the Betts-Ditzian value and our value. The disagreement is, however, in the fourth place and thus should not affect the analysis. We believe that our value is correct. We thank Dr. Ruth V. Ditzian for useful correspondence on this point.

⁷J. W. Essam and M. F. Sykes, *Physica* **29**, 378 (1963). In calculating the $S = \frac{1}{2}$ Ising model series we have reproduced the HTS coefficients for the susceptibility and specific heat series given by Essam and Sykes. Our coefficients for the second moment series are, however, a new result. By comparing Essam and Sykes' 16th-order series results with our tenth-order result on the $S = \frac{1}{2}$ Ising model, we obtain a qualitative understanding of how the series for the other models should behave.

⁸For a description of the entire spinel structure and comments on relevance to magnetic materials, see K. Dwight and N. Menyuk, *J. Appl. Phys.* **39**, 660 (1968); *Phys. Rev.* **163**, 435 (1967) and also references therein.

⁹If one compares the illustrations for the lattices given in Refs. 5, 6, and 8, it is easy to appreciate why the B sites of the spinel lattice, AB_2X_4 , were not immediately recognized as the B sites of the cristobalite lattice, AB_2 .

¹⁰Figure 1 shows the AB_2 cristobalite lattice. The A sites of this lattice do not occupy the same position as the A sites of the spinel lattice.

¹¹A "self-avoiding walk" is a walk from site to site without stepping on a site which has previously been visited. We ask how many steps are necessary to form the smallest closed loop. For the sc and bcc lattices this number is 4 while for the fcc and B-site spinel this number is 3. This corresponds to the

comments in the text concerning the triangular graphs.

¹²R. W. Gibberd, *Can. J. Phys.* **48**, 307 (1969).

¹³M. Wortis, D. Jasnow, and M. A. Moore, *Phys. Rev.* **185**, 805 (1969).

¹⁴Our correlation functions are defined with respect to the strong directions. For example, for the X-Y model, by $C_2(\mathbf{r})$ we refer to $\langle S_0^x S_r^x \rangle$ or $\langle S_0^y S_r^y \rangle$ and not to $\langle S_0^x S_r^y \rangle$.

¹⁵Reference 7. Also for HTS with arbitrary second-nearest-neighbor interactions on the diamond lattice, see P. Horn, R. Parks, D. N. Lambeth, and H. E. Stanley, *Phys. Rev. B* **9**, 316 (1974).

¹⁶For a review of methods of series analysis see G. A. Baker, Jr., and D. L. Hunter, *Phys. Rev. B* **7**, 3346 (1973) and

references contained therein.

¹⁷On a more tightly packed lattice these ratio plots ($n=D$) should not be so erratic. Hence, the similarities would not be expected to be displayed so dramatically.

¹⁸In the Padé approximant tables D and N refer to the orders of the polynomials in the denominator and numerator, respectively.

¹⁹M. H. Lee and H. E. Stanley, *Phys. Rev. B* **4**, 1613 (1971); also see D. D. Betts, C. J. Elliott, and R. V. Ditzian, *Can. J. Phys.* **49**, 1327 (1971). For a previous analysis of some eighth-order spinel series using the transformation of Eq. (4.4) see M. H. Lee and H. E. Stanley, *J. Phys. (Paris)* **32S**, 352 (1971).